RESEARCH ARTICLE

Effect of increased pCO_2 on bacterial assemblage shifts in response to glucose addition in Fram Strait seawater mesocosms

Jessica L. Ray[1,2], Birte Töpper[2], Shu An[3], Anna Silyakova[4,5], Joachim Spindelböck[2,6], Runar Thyrhaug[2†], Michael S. DuBow[3], T. Frede Thingstad[2] & Ruth-Anne Sandaa[2]

[1]Uni Environment, Uni Research AS, Bergen, Norway; [2]Department of Biology, University of Bergen, Bergen, Norway; [3]CNRS UMR 8621, Institut de Génétique et Microbiologie, Univ Paris-Sud, Orsay, France; [4]Uni Bjerknes Centre, Bergen, Norway; [5]Bjerknes Centre for Climate Research, Bergen, Norway; and [6]Sogn og Fjordane University College, Sogndal, Norway

Correspondence: Jessica L. Ray, Uni Environment, Uni Research AS, Postboks 7810, N-5020 Bergen, Norway.
Tel.: (+47) 55 58 84 19;
fax: (+47) 55 58 44 50;
e-mail: jessicalouiseray@gmail.com

[†]Deceased.

Received 16 April 2012; revised 20 June 2012; accepted 29 June 2012.
Final version published online 6 August 2012.

DOI: 10.1111/j.1574-6941.2012.01443.x

Editor: Gary King

Keywords
glucose; pyrosequencing; acidification; Fram Strait; bacteria; V1-V2 16S rDNA amplicon library.

Abstract

Ocean acidification may stimulate primary production through increased availability of inorganic carbon in the photic zone, which may in turn change the biogenic flux of dissolved organic carbon (DOC) and the growth potential of heterotrophic bacteria. To investigate the effects of ocean acidification on marine bacterial assemblages, a two-by-three factorial mescosom experiment was conducted using surface sea water from the East Greenland Current in Fram Strait. Pyrosequencing of the V1-V2 region of bacterial 16S ribosomal RNA genes was used to investigate differences in the endpoint (Day 9) composition of bacterial assemblages in mineral nutrient-replete mesocosms amended with glucose (0 μM, 5.3 μM and 15.9 μM) under ambient (250 μatm) or acidified (400 μatm) partial pressures of CO_2 (pCO_2). All mesocosms showed low richness and diversity by Chao1 estimator and Shannon index, respectively, with general dominance by Gammaproteobacteria and Flavobacteria. Nonmetric multidimensional scaling analysis and two-way analysis of variance of the Jaccard dissimilarity matrix (97% similarity cut-off) demonstrated that the significant community shift between 0 μM and 15.9 μM glucose addition at 250 μatm pCO_2 was eliminated at 400 μatm pCO_2. These results suggest that the response potential of marine bacteria to DOC input may be altered under acidified conditions.

Introduction

During the last few decades, atmospheric carbon dioxide (CO_2) has increased because of anthropogenic activity, and it is predicted to continue increasing for the foreseeable future (IPCC 'Business as Usual' scenario IS92a). As atmospheric CO_2 is in equilibrium with CO_2 in the surface layer of the ocean, increased atmospheric CO_2 leads to increased CO_2 in the ocean and changes the oceanic carbon chemistry, resulting in acidification (Caldeira & Wickett, 2003). It is also thought that elevated oceanic partial pressure of CO_2 (pCO_2) promotes higher carbon incorporation through photosynthesis (primary production) with the consequence that increasing concentrations of phytoplankton-derived dissolved organic carbon (DOC) compounds are released into the water column (Engel *et al.*, 2004; Riebesell *et al.*, 2007) with the potential consequence of stimulating carbon overconsumption in the photic zone (Toggweiler, 1993). Heterotrophic bacteria are the most important consumers of DOC in aquatic ecosystems (Amon, 2004) and might therefore be directly or indirectly affected by acidification-induced increases in DOC (Beman *et al.*, 2011).

Several studies have already reported the strong response of marine bacteria to an increase in DOC in the form of glucose (Øvreås *et al.*, 2003; Elifantz *et al.*, 2005; Malmstrom *et al.*, 2005; Alonso & Pernthaler, 2006; Töpper *et al.*, 2010). Although glucose accounts for < 1% of bulk DOC (Nagata, 2008), it is the most abundant free neutral sugar in sea water. Glucose has

FEMS MICROBIOLOGY ECOLOGY

been reported to support a high percentage of bacterial production (Rich *et al.*, 1996), with low concentrations (0.1–100 nM) favouring the growth of Alphaproteobacteria (Malmstrom *et al.*, 2005; Alonso & Pernthaler, 2006; Alonso-Sáez & Gasol, 2007), while high concentrations (40–763 μM) favour the growth of Gammaproteobacteria (Øvreås *et al.*, 2003; Pinhassi & Berman, 2003). Both bacterial abundance and assemblage structures can change in response to glucose manipulation, although the development of the bacterial assemblage seems to strongly depend on the initial structure and nutrient state of the system under investigation (mineral nutrient- or carbon-limited) at the time of glucose amendment (Thingstad *et al.*, 2008).

Bacterial growth also requires mineral nutrients (i.e. nitrate and phosphate), which may be of limited availability in the ocean surface layer, and may vary independently of fluctuations in DOC concentration. Inhibition of bacterial DOC-utilisation by mineral nutrient limitation might promote DOC accumulation in the upper ocean (Thingstad *et al.*, 1997) with the potential to enhance the efficacy of the carbon pump for organic matter transport to the deep ocean. If acidification because of increased pCO_2 in the ocean results in increased rates of C-fixation via photosynthesis, and thereby greater downward C-transport because of surface-layer nutrient limitation of heterotrophic C-utilisation, it becomes critically important to understand the potential impacts of increased oceanic pCO_2 on heterotrophic C-utilisation to determine how the biological carbon pump will be affected, or how acidification itself might affect marine bacterial assemblages and their ability to utilise DOC, particularly under conditions of elevated primary production leading to increased availability of DOC.

Fram Strait acts as a gateway for the flow of North Atlantic sea water into the Arctic Ocean in the eastern side and for the exit of sea water from the Arctic Ocean on the western side. Fram Strait is thus the key area for exchange of the water masses, and subsequently organic matter, between the North Atlantic and the Arctic Oceans. Circulation patterns and water mass exchange in Fram Strait create a strong gradient between warm and cold waters. In addition, there is a marginal sea ice zone characterised by enhanced biological activity, including primary production (Smith & Nelson, 1990). Complex oceanographic conditions in Fram Strait allow intense interaction between plankton communities in different seasonal stages, which provides an ideal system for investigation of trophic interactions (Hirche *et al.*, 1991). Examination of the effects of ocean acidification using seawater microbial assemblages present in Fram Strait can provide a glimpse into the potential effects of rising pCO_2 on interactions between bacterial and plankton communities, which are very important for the trophic interactions and the function of the biological pump in this area.

In this study, we have combined the experimental advantages of seawater mesocosms with the resolution of pyrophosphate sequencing (pyrosequencing) to address the important question of how ocean acidification might impact the bacterial component of the biological carbon pump in highly productive sea water of Fram Strait. More specifically, we wished to test whether artificial acidification of seawater mesocosms will affect bacterial assemblage shifts in response to an increased organic carbon load.

Materials and methods

Geographic coordinates of sampling site

The mesocosm experiment was performed on the open deck of the research vessel G.O. Sars (Institute for Marine Research and the University of Bergen, Norway) during June 2009. The study site was located in Fram Strait at 76.93°N, 3.58°W, between the eastern coast of Greenland and the Svalbard archipelago. This location was chosen to allow sampling of surface sea water exiting the Arctic Ocean via the East Greenland current. Water from 6 m depth was pumped into a holding tank on board the ship, where it was allowed to settle for 1 day prior to distribution into six polyethylene tanks with a volume of 1 m^3.

Three mesocosms with present pCO_2 levels ('P') were not CO_2-manipulated and had a mean pCO_2 of 250 μatm. In the three remaining mesocosms, the CO_2 balance was artificially perturbed by the addition of HCl and $NaHCO_3$ such that the pCO_2 was increased to 400 μatm without an increase in net alkalinity (Gattuso & Lavigne, 2009). These mesocosms were referred to as future pCO_2 mesocosms ('F') in the sense that they were manipulated to create increased pCO_2 levels over ambient conditions, a situation that is predicted to occur in a future acidified ocean environment. One mesocosm from both pCO_2 levels received daily additions of either no glucose ('0'), 5.3 μM glucose (1X-Redfield ratio, '1') or 15.9 μM glucose (3X-Redfield ratio, '3'). This resulted in a two-by-three factorial design to test two different pCO_2 concentrations and three different glucose concentrations (mesocosms P0, P1, P3, F0, F1 and F3). All mesocosms were kept mineral nutrient replete by daily additions of 0.8 μM $NaNO_3$, 0.05 μM KH_2PO_4 and 0.8 μM $NaSiO_4$ (N:P:Si = 16:1:16). Mesocosms were gently mixed with an aquarium pump for 30 min prior to daily samplings. As mesocosm tanks were sealed with lids to limit gas exchange with the atmosphere, sampling was conducted

via clamp-sealed silicon tubing mounted through the tank lids. Seawater samples were siphoned from the middle of each tank, after which the tubing was immediately resealed to prevent unwanted gas exchange between the mesocosms and atmosphere. The experiment was conducted from 20 to 29 June 2009 (Day 0–Day 9). Physical and chemical parameters of Day 9 mesocosm sea water are given in Table S1 (Supporting Information).

Flow cytometry

Phytoplankton and bacterial counts were determined by flow cytometry using a FACS Calibur (Beckton Dickinson) equipped with a 15 mW 488 nm air-cooled laser and standard filter set (Marie *et al.*, 1999). Phytoplankton were enumerated by discrimination of chlorophyll autofluorescence and side scatter signals in fresh samples. Phytoplankton counts include all size and pigment classes of phytoplankton < 20 μm in diameter: picophytoplankton (Prasinophyceae and cyanobacteria), nanophytoplankton (e.g. haptophytes), coccolithophorids (e.g. *Emiliania huxleyi*), and dinoflagellates (Cryptophyceae), while chain forms of diatoms were likely excluded from counts. Samples for bacterial counts were fixed with 1% (v/v) glutaraldehyde for 30 min at 4 °C in the dark, diluted in sterile 0.2 μm-filtered 10 mM Tris-Cl, 1 mM NaEDTA buffer (pH 8.0) (1× TE buffer) then stained with 1× SYBR Green I at room temperature for 20 min. Appropriate dilutions were counted with discriminator set to green fluorescence.

Filtration and DNA extraction

On the final day of the experiment (Day 9, 29 June 2009), bacteria in 340–500 mL of sea water from each mesocosm were collected by vacuum filtration onto sterile 0.2 μm pore size SUPPOR filters (Pall Life Sciences, Ann Arbor, MI). The filters were aseptically placed into sterile cryostorage tubes, frozen in liquid nitrogen and stored at −80 °C until processing. Nucleic acids were isolated from filters using a modified protocol for alkaline-SDS lysis followed by hexadecyltrimethylammonium bromide (CTAB) purification (Töpper *et al.*, 2010).

V1-V2 16S rDNA amplification and bacterial tag-encoded FLX amplicon pyrosequencing (bTEFLXAP)

An aliquot of extracted total DNA was adjusted to a final DNA concentration of 15 ng μL^{-1} in 0.1× TE buffer using a NanoVue spectrophotometer (GE Healthcare, Velizy-Villacoublay, France) and verified by ethidium bromide fluorescence after electrophoresis on a 1% agarose gel in 1× TAE (2 mM Tris-acetate pH 8.0, 5 mM NaEDTA) buffer. Then, multiple 50-μL polymerase chain reactions (PCRs) were performed using the universal 16S rRNA gene bacterial primers 8F (BxxxxxxAGAGTTTGATCM TGGCTCAG) and 357R (AxxxxxxCTGCTGCCTYCC GTA), where B and A represent the adaptors B and A for pyrosequencing using the Gold reaction (GS20, Roche/454 Life Sciences). The xxxxxx represents six-nucleotide (nt) sequence tags designed for sample identification barcoding. PCR amplification conditions were adapted for the use of two different thermostable DNA polymerases: (1) Phusion High-Fidelity DNA Polymerase (Finnzymes Oy, Vantaa, Finland): 98 °C for 2 min followed by 25 cycles of 98 °C for 30 s, 48 °C for 20 s and 72 °C for 12 s and a final elongation step at 72 °C for 5 min; (2) Pfu DNA Polymerase (Fermentas): 95 °C for 3 min followed by 35 cycles of 95 °C for 30 s, 48°C for 30 s and 72 °C for 48 s and a final elongation step at 72 °C for 5 min. Each 50-μL PCR mixture contained 15 ng DNA, 0.1 μM of each primer (Sigma-Aldrich), 0.2 mM dNTP mix (Fermentas) and 1.25 units polymerase using the buffers supplied with each polymerase. Each DNA sample was subjected to 5–10 replicate PCRs per thermostable DNA polymerase. The resulting PCR products from all replicate reactions for both polymerases were pooled and loaded on a 1% agarose gel in 1× TAE buffer. After DNA visualisation by ethidium bromide staining and long-wave UV light illumination, the amplified V1-V2 16S rRNA gene fragments were excised from the gel and purified using the NucleoSpin Extract II kit (Macherey-Nagel, Hoerd, France) according to manufacturer instructions. Fifty nanograms of PCR products from each sample were pooled for pyrosequencing runs. Pyrosequencing was performed using a Roche/454 FLX Pyrosequencer (GATC Biotech, Konstanz, Germany). The sequences obtained for each sample were grouped according to the tag used and, after removal of the tags, the average sequence length was calculated to be 227 nt.

Sequencing data analysis

Using the Ribosomal Database Project II (RDP-II) pyrosequencing pipeline (http://pyro.cme.msu.edu/index.jsp) (Cole *et al.*, 2009), sequences were filtered based on minimum length of 150 nt, a maximum of two errors within the primer binding site and a minimum average quality score of 25 over 90% of the sequence. Potential chimeric 16S rRNA gene sequences were identified from individual data sets using the freely-available Black Box Chimera Check (B2C2) program (Gontcharova *et al.*, 2010). We were unable to corroborate B2C2 identification of chimeric sequences by manual BLAST analysis of 3′- and 5′-end of sequences, but as the frequency of chimeras

was very low for all mesocosm data sets (Table 1), we chose to exclude these sequences from further analyses. Sequences were then classified using RDP-II Classifier set to the default confidence threshold value (80%). The Chao1 estimator of sample richness and Shannon index of diversity were also calculated using the RDP-II pyrosequencing pipeline. Sequences have been deposited as Sequence Read Archive ERP001357 (http://www.ebi.ac.uk/ena/data/view/ERP001357).

Statistics

As this study is a first attempt to use pyrosequencing analysis of mesocosm samples, we did not consider replicate mesocosms for the treatments. Taking advantage of the large data sets generated by pyrosequencing, however, we increased the statistical resolving power of our diversity analyses by dividing individual sequencing data sets into five pseudoreplicate sub-data sets without resampling. In this way, each sequence is only represented once in statistical analyses, thus preserving the true diversity in undivided data sets. The sequencing data sets for each mesocosm were randomly divided into five subsets of equal size using the Perl script fastarandsplitter.pl (Michael Dondrup, Uni Computing CBU, Bergen, Norway) and labelled accordingly, for example, P0-1, P0-2…P0-5. One subset from each treatment was combined with the same numerical subset from all other treatments to generate five sub-data sets, each containing one sequencing subset from each of the six treatments. Alignment and complete linkage clustering analysis with a 3% dissimilarity cut-off (RDP-II) (Kunin *et al.*, 2010) were performed on each of the five sub-data sets, and Jaccard distance tables were calculated from the results. For intersample comparisons of bacterial diversity, we deliberately chose the Jaccard similarity index, which looks only at presence–absence data for each operational taxonomic units (OTU), rather than the Bray–Curtis index, which takes into account both OTU richness and evenness, as we were concerned that the low evenness in all samples would mask the contribution of taxa richness to community diversity. Euclidean distances were therefore calculated from a Jaccard dissimilarity matrix for all sub-data sets and all treatments and plotted using nonmetric multidimensional scaling analysis (NMDS) in SPSS (IBM).

To test the hypothesis that ocean acidification has significant effect on bacterial assemblage profile shifts in response to glucose addition, we performed two-way analysis of variance (ANOVA) on Jaccard dissimilarity values for nonglucose amended mesocosms (P0 or F0) with the two different levels of glucose amendment (P1/F1 or P3/F3) using a linear mixed-effects model (see Pinheiro & Bates, 2000 for details) to account for the pseudoreplication issued from the five data subsets. We parameterised the model with Jaccard dissimilarity value as response variable, glucose and pCO_2 treatments as explanatory variables and mesocosm comparisons as random effects. The analysis was performed with the function lmer in the R package lme4 (R Development Core Team, 2005; Bates *et al.*, 2012). An lmer model does not provide *P*-values on its model estimates (Hornik, 2012), so we used maximum likelihood tests to assess the significance of each term's contribution to the model. The so-obtained *P*-values are indicated as P_{ML} (Table 2). To test the assumptions of normality of errors and constancy of error variance, we used the Shapiro–Wilk test and the Levene's test, respectively.

Results

Flow cytometric enumeration of bacteria and microalgae (Fig. 1) demonstrated an increase in bacterial numbers in

Table 1. Pyrosequencing metrics and diversity indices for 0.2-μm-filtered bacterial assemblages sampled from 340 to 500 mL of mesocosm water on the last experimental day (Day 9)

Sample	Raw*	Trimmed†	Not chimera‡	OTUs§	Chao1¶	OTU/Chao1**	H′††
P0	5809	4123	4107	76	126	60.3	2.3
P1	7635	5271	5243	67	75	89.3	2.2
P3	4167	3085	3079	65	107	60.7	2.3
F0	7315	4933	4930	44	70	62.9	1.4
F1	4161	3197	3180	67	96	69.8	2.3
F3	6301	4999	4977	85	108	78.7	2.0

*Raw, the total number of raw 16S ribosomal RNA (rRNA) gene sequences reads generated.

†Trimmed, the number of raw sequence reads fulfilling requirements for sequence quality (see Materials and Methods).

‡Not chimera, the number of sequences designated as nonchimeric by the B2C2-program check for chimeric 16S rRNA amplicons.

§OTUs, the number of operational taxonomic units (OTUs) identified using a 97% sequence similarity cut-off.

¶Chao1, Chao1 estimator of OTU richness (97% similarity cut-off).

**OTU/Chao1, the percentage of Chao1-estimated OTU richness represented by sequence data set.

††H′, Shannon index of OTU diversity (97% sequence similarity cut-off).

Table 2. Fixed effect statistics for the lmer model on glucose amendments under two pCO_2 treatments

Comparison	Estimate*	SE	*t* Value	P_{ML}
Intercept (P0–P1)	0.1229	0.04559	2.70	< 0.001
Difference P0–P1 to P0–P3	0.38106	0.06448	5.91	< 0.001
Difference P0–P1 to F0–F1	−0.01415	0.06448	−0.22	> 0.05
Difference F0–F1 to F0–F3	−0.34652	0.09119	−3.80	< 0.001

*Diversity estimates based on Jaccard dissimilarity with 3% cut-off.

all mesocosms up to Day 3 of the experiment, with bacterial numbers peaking at around 1.5×10^6 bacterial mL^{-1} in all mesocosms except mesocosm P3. In this mesocosm, Day 3 bacterial counts were marked by a sharp decline to 7.6×10^5 bacteria mL^{-1}. By Day 4, however, bacterial numbers in this mesocosm (1.2×10^6 bacteria mL^{-1}) were again similar to bacterial numbers observed in the other mesocosms. In all mesocosms, bacterial numbers decreased between Day 4 and Day 9, ending at approximately 4×10^5 bacteria mL^{-1}, whereas initial numbers of phytoplankton were about 1.5×10^4 cells mL^{-1} (Fig. 1). In all mesocosms, phytoplankton numbers increased up to Day 4 ($2.5–3.0 \times 10^4$ cells mL^{-1}), except in mesocosm P3 (Fig. 1), where phytoplankton numbers dropped abruptly to ~1.5×10^4 cells mL^{-1}. Phytoplankton numbers in all treatments decreased between Day 4 and Day 9, dropping to $\leq 1.0 \times 10^4$ cells mL^{-1} by the conclusion of the experiment.

Pyrosequencing of 16S rRNA gene amplicons using the reverse primer only (primer 357R) resulted in the generation of 35388 raw sequences in total (Table 1), with a mean of 5898 ± 1222 sequences per sample. Quality-trimming and chimera checks resulted in removal of 1645 ± 627 sequences per sequence data set (Table 1). A total of 25 516 sequences were subsequently analysed using the RDP-II pyrosequencing pipeline for taxonomic classification, alignment and cluster analysis. The total number of sequences analysed per mesocosm sample varied from 3079 sequences (mesocosm P3) to 5243 sequences (mesocosm P1) (Table 1). All sequences were identified as bacterial using the RDP-II Classifier (data not shown).

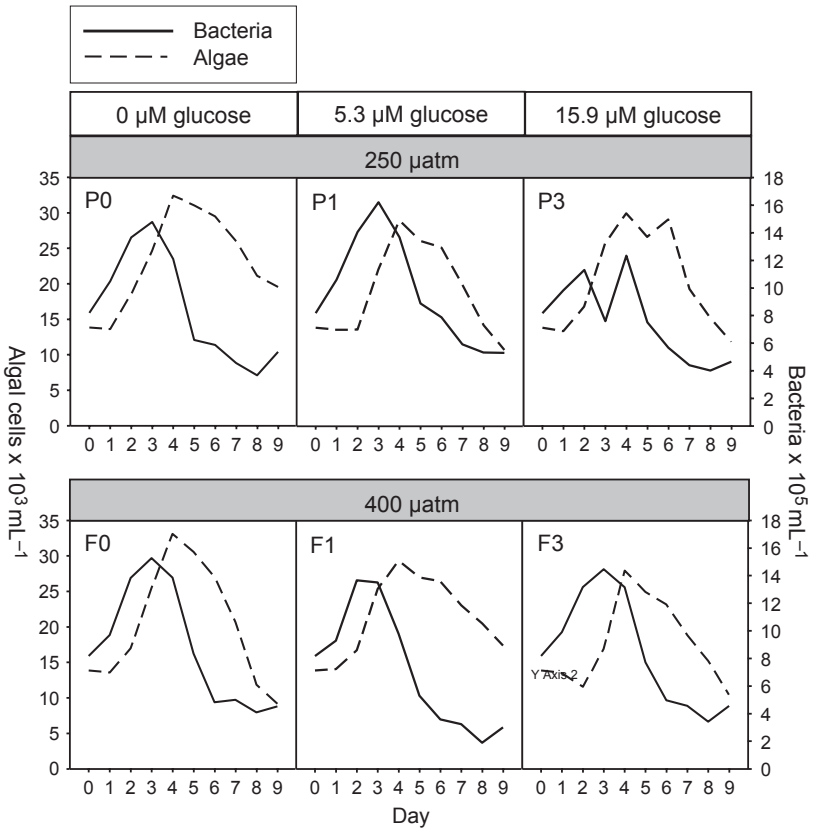

Fig. 1. Total bacteria (solid line) and phytoplankton ($\leq$ 20 µm, dashed line) abundance determined by flow cytometry. P0, 250 µatm pCO_2 and no glucose addition; P1, 250 µatm pCO_2 and 1X-Redfield ratio glucose addition; P3, 250 µatm pCO_2 and 3X-Redfield ratio glucose addition; F0; 400 µatm pCO_2 and no glucose addition; F1; 400 µatm pCO_2 and 1X-Redfield ratio glucose addition; F3; 400 µatm pCO_2 and 3X-Redfield ratio glucose addition.

Rarefaction analysis of sequence libraries for each mesocosm (Fig. 2) demonstrated low richness for all mesocosms despite the relatively low number of sequences analysed. In particular, the rarefaction curve for mesocosm F0 predicted saturation of OTU at approximately 50 OTU based on 3% dissimilarity cut-off. Concordant with the rarefaction analysis, Chao1 estimates and Shannon diversity indices for each mesocosm (Table 1) showed low richness and diversity in general, with no clear trend suggesting increase or decrease in assemblage diversity because of pCO_2 or glucose manipulation, although the relatively low Chao1 and Shannon indices for the F0 mesocosm (Table 1) in particular suggest a decrease in bacterial community richness and diversity because of acidification treatment in the absence of glucose addition. Ratios of the number of OTU observed to Chao1 estimates demonstrate that the sequence data sets represent 60–90% of the Chao1-predicted OTU richness for each sample (Table 1).

Taxonomic classification of sequencing reads at the class (Fig. 3a) and family (Fig. 3b) levels revealed differences in OTU diversity between pCO_2 treatments and glucose treatments. Alphaproteobacteria, in particular in the family Rhodobacteraceae, showed the highest abundance in the P3 mesocosm relative to all other mesocosms and were notably absent in the F0 mesocosm. Flavobacteria (family Flavobacteriaceae) exhibited decreasing relative abundance with increasing glucose addition in the P mesocosms, but the opposite trend in the F mesocosms. The relative abundance of Gammaproteobacteria in the P mescosms was slightly higher at the Redfield ratio for glucose-C (P1) than at the 0 μM (P0) or 15.9 μM (P3) glucose additions (Fig. 3). In the F mesocosms, we observed

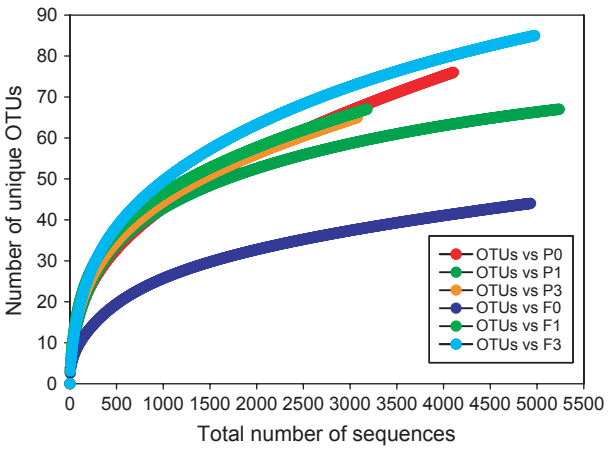

Fig. 2. Rarefaction analysis of trimmed, quality- and chimera-checked pyrosequencing data sets for the six mesocosms. OTU determination was based on a 97% sequence similarity cut-off. Meosocosm designations are as described in Fig. 1.

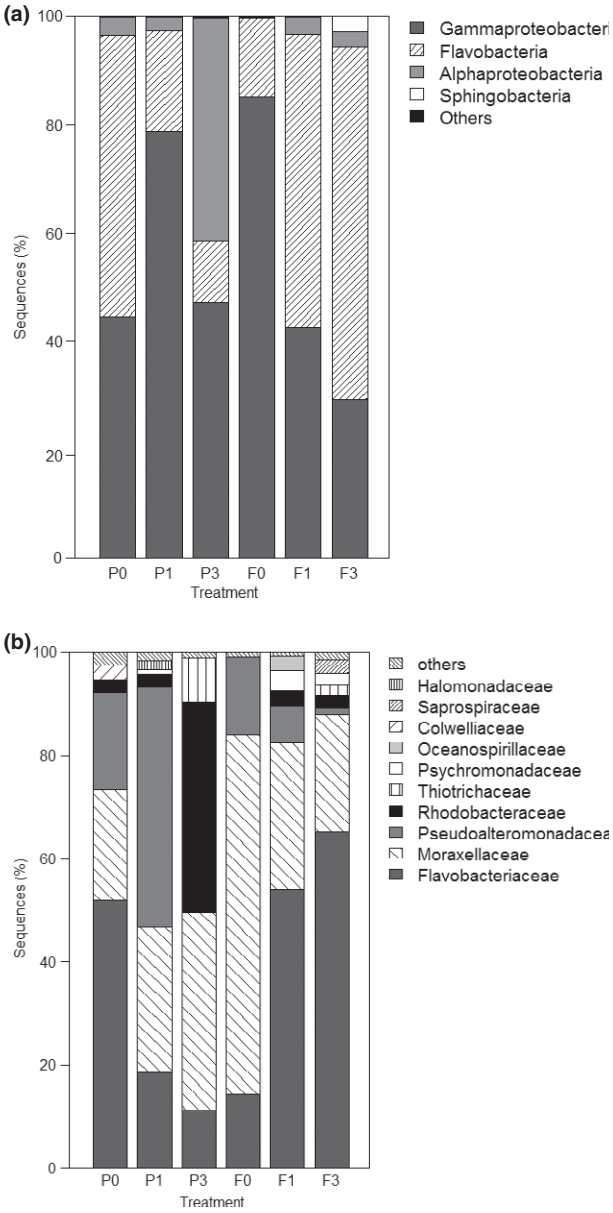

Fig. 3. Taxonomic composition based on relative percentage of total 16S ribosomal RNA amplicon pyrosequencing reads from individual mesocosms. Classification was performed using the RDP-II Classifier set to default parameters at (a) class and (b) family level. Reads that accounted for < 1% of total reads for each data set were pooled into 'Others'.

a decline in relative abundance of Gammaproteobacteria with increasing glucose addition. The Gammaproteobacterial families responding most prominently to treatment were Pseudoalteromonadaceae and Moraxellaceae. In the P mesocosms, the relative abundance of Pseudoalteromonadaceae increased greatly in mesocosm P1 relative to P0, but was very low in mesocosm P3. In the F mesocosms, Pseudoalteromonadaceae abundance decreased with

increasing glucose concentration. For the Moraxellaceae, relative abundance increased with increasing glucose concentration in the P mesocosms, but decreased with increasing glucose concentration in the F mesocosms. In addition to these generally dominant bacterial groups, some bacterial taxa were rare or only sporadically identified among the six mesocosm samples examined. Sphingobacteria (family Saprospiraceae), for example, were found in noteworthy numbers only in the F3 mesocosm, in which they comprised 2.79% of total sequencing reads (Fig. 3a). Acintobacteria, Betaproteobacteria, Bacilli and Verrumicrobia were identified in many of the sequence data sets, although each accounted for no more than seven sequencing reads in any sample.

The use of nonmetric multidimensional scaling to plot Euclidean distances between all different mesocosms revealed that shifts in bacterial assemblage structures were dependent upon glucose addition (Fig. 4). The lmer model of Jaccard dissimilarity values for the glucose and pCO_2 treatments revealed that the shift in bacterial assemblage structure from P0 to P1 was fourfold smaller ($P_{ML} < 0.001$, see Table 2) than the shift from P0 to P3. At elevated pCO_2, the shift in bacterial assemblage structure from F0 to F1 was not different from that observed for P0 to P1 ($P_{ML} > 0.05$). For the F0 to F3 comparison, however, we found that the dramatic shift in bacterial assemblage structure observed from P0 to P3 was eliminated at elevated pCO_2 ($P_{ML} < 0.001$).

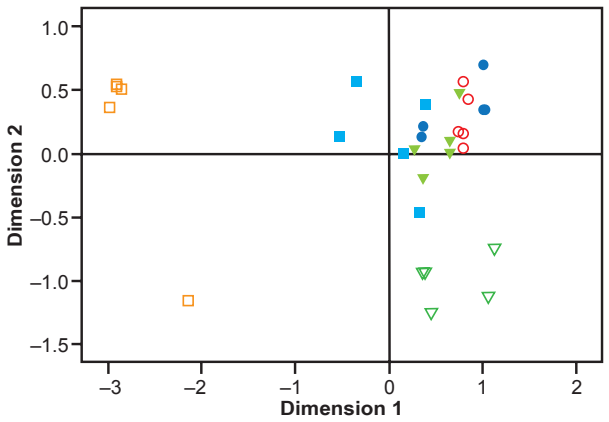

Fig. 4. Non-metric multidimensional scaling analysis of Jaccard dissimilarity values (3% cut-off) for five sequence subsets from all six mesocosms. Open red circles, P0, dark green open triangles; P1, orange open squares; P3, blue solid circles; F0, light green solid triangles; F1, turquoise solid squares, F3. Description of mesocosm treatments is the same as for Fig. 1. Stress = 0.00286, RSQ = 0.99996.

Discussion

We have utilised second-generation sequencing technology in combination with seawater mesocosm manipulations to test the effects of pCO_2 manipulation on changes in the structure of indigenous Arctic marine bacterial assemblages in response to increasing DOM input. These data demonstrate a statistically significant interaction between bacterial assemblage responses to high DOM input and their response to seawater acidification. In particular, we show that shifts in bacterial assemblage structure because of excess DOC in the form of glucose were reduced after 9 days in acidified seawater mesocosms relative to nonacidified mesocosms. Our results suggest that the role of Arctic marine bacterial assemblages in organic carbon turnover in the ocean may be affected by ocean acidification, although investigation of the exact responses of bacteria to increased DOC under artificially 'acidified' conditions falls outside the scope of the present study. To our knowledge, this is the first description of pyrosequencing of mesocosm samples for deeper examination of marine bacterial assemblage responses to high glucose addition under acidified conditions. We found this combination to be a powerful tool for investigation of the effects of experimental manipulations on microbial communities.

The IPCC 'business as usual' scenario (IS92a) reports that the current global atmospheric CO_2 concentration is 380 μatm, but is predicted to increase to 700 μatm CO_2 by 2100. In the current study, mesocosms with and without experimental pCO_2 manipulation resulted in mean pCO_2 values of 250 μatm in the P mesocosms and 400 μatm in the F mesocosms, respectively. The discrepancy between the IPCC-reported values and the experimental values reported in this study is most likely due to the naturally lower pCO_2 in Arctic water relative to the global ocean mean, particularly post–spring bloom when drawdown of CO_2 because of photosynthetic activity results in low pCO_2 (Bates & Mathis, 2009). The experimental pCO_2 values in this study therefore represent ambient and increased pCO_2 levels as a proxy for testing the effects of ocean acidification on Arctic marine bacterial responses to DOM input.

Sequences present in the data sets from mesocosm samples have high similarity ($\geq$ 97%) to sequences previously identified in Arctic and North Sea marine environments (Eilers *et al.*, 2000a; Malmstrom *et al.*, 2007; Kirchman *et al.*, 2010), albeit at variable relative abundances. Gammaproteobacteria and Flavobacteria were clearly dominant in our mesocosms (Fig. 3a). Closely related taxa have previously been identified in sequencing studies of sea water (Bano & Hollibaugh, 2002; Alonso *et al.*, 2007; Galand *et al.*, 2009) and have

also been observed to respond rapidly to nutrient additions and cultivation attempts (Eilers *et al.*, 2000b; Fuchs *et al.*, 2000; Pinhassi *et al.*, 2006; Witt *et al.*, 2011). One study of North Sea bacterial assemblages, however, revealed that the Pseudoalteromonadaceae family of Gammaproteobacteria, which were dominant in several mesocosms in this study, were rarely present in environmental samples yet were readily culturable (Eilers *et al.*, 2000a). Indeed, rapid shifts in bacterial assemblage composition in response to confinement have been reported (Ferguson *et al.*, 1984; Fuchs *et al.*, 2000; Massana *et al.*, 2001; Allers *et al.*, 2007), therefore we cannot exclude the likelihood that treatment and incubation effects may have significantly altered the development of bacterial assemblages in mesocosms relative to a natural response in the marine environment. We do not suggest that the bacterial assemblage shifts demonstrated here are reflections of bacterial assemblage responses *in situ*, but have rather chosen to interpret our results as an indicator of the response potential that exists within natural bacterial assemblages in Fram Strait surface sea water.

The generally low bacterial diversity in our samples is corroborated by previous studies of seawater bacterial assemblages, particularly at high latitudes (Malmstrom *et al.*, 2007; Pommier *et al.*, 2007; Fuhrman *et al.*, 2008; Pommier *et al.*, 2010). Diversity comparisons between the different mesocosm treatments were therefore challenging, as calculated diversity indices lay within a very narrow range (Table 1). Chao1 estimators would seem to suggest that glucose addition at three times the Redfield ratio (in mesocosms P3 and F3) caused a slight relative increase in bacterial assemblage diversity at the 97% similarity level (Table 1) relative to the lower glucose amendments, although we were unable to confirm this trend with any statistical confidence. Assuming low diversity of bacteria in the source sea water for the experiment, we may speculate that diversity might further decrease during the 9-day experimental period because of treatment effects (Øvreås *et al.*, 2003). As the initial bacterial diversity in sea water at the sampling site was not assessed, it is not possible to conclude whether the dominance observed in Day 9 samples was attributed to experimental manipulation or is a reflection of natural dominance in surface sea water in this region.

The significant bacterial assemblage shift between the P0 and P3 mesocosms (Table 2) corroborates previous findings that organic carbon addition stimulates community shifts both in laboratory experiments (Massana *et al.*, 2001; Malmstrom *et al.*, 2005; Alonso & Pernthaler, 2006; Alonso-Sáez & Gasol, 2007; Töpper *et al.*, unpublished results) as well as in mesocosms (Øvreås *et al.*, 2003; Sandaa *et al.*, 2009; Töpper *et al.*, 2010). These community shifts are often characterised by relative increases in Gammaproteobacteria (Eilers *et al.*, 2000a, b; Fuchs *et al.*, 2000; Øvreås *et al.*, 2003), which were abundant in all our mesocosms (Fig. 3a). We observed a relative increase in Flavobacteria in the F3 mesocosm relative to F0 or F1 mesocosms (Fig. 3a), which is in agreement with observations that this bacterial class responds positively to increased pCO_2 in the presence of added DOC (Witt *et al.*, 2011). Interestingly, we observed a negative relationship between glucose addition and relative contribution of Flavobacteria to bacterial assemblages in the P mesocosms, suggesting the importance of the interaction between pCO_2 and DOC for Flavobacterial proliferation during this experiment. As numerically dominant bacteria are thought to be the most active members of bacterial assemblages (Cottrell & Kirchman, 2003; Andersson *et al.*, 2010; but see also Alonso & Pernthaler, 2006), we cautiously conclude that Gammaproteobacteria responded negatively, while Flavobacteria responded positively (Witt *et al.*, 2011) to acidification when glucose addition rates were at or in excess of the Redfield ratio. More ambitious generalisations about bacterial group responses to experimental treatments at such low taxonomic resolution would be unwise, as previous research has documented the broad potential diversity of bacterial responses at or above the family taxonomic level (Eilers *et al.*, 2000b; Allers *et al.*, 2007).

Our finding that the change in bacterial assemblage structure in response to high glucose addition under present pCO_2 (mesocosm P3) was eliminated under acidified conditions (mesocosm F3) is noteworthy. As the significant difference between the bacterial assemblages in the P and F mesocosms was identified between the no-glucose to the high-glucose treatments (P0 to P3 vs. F0 to F3), we conclude that the specific effect of pCO_2 on bacterial assemblage structures is connected to the variable ability of heterotrophic bacteria to utilise glucose over the Redfield ratio of N and P under normal and acidified conditions. Bacterial uptake of DOC over the Redfield ratio has been observed previously for marine bacteria that apparently store excess carbon in C-rich inclusion bodies (Øvreås *et al.*, 2003), although that mesocosm experiment was conducted at ambient pCO_2. TEM analysis of bacteria was not performed for the current mesocosm experiment; therefore, it remains unknown whether natural marine bacterial assemblages utilise such a 'Winnie-the-Pooh' strategy (Thingstad *et al.*, 2005, 2010). It is additionally unclear whether acidification could somehow inhibit such a storage strategy or whether it might alter carbon substrate affinity or preference among heterotrophic bacteria. We must also take into consideration that acid–base manipulation of sea water carbonate chemistry, as opposed to CO_2 bubbling, to increase pCO_2 levels may have influenced the outcome of the study.

Further research is clearly required to more precisely examine the biochemical and physiological effects of experimental acidification on C-assimilation rates in marine bacteria.

We do not feel it likely that the acidification effect described here is attributed to generic physiological inhibition of bacterial activity in acidified mesocosms (F0, F1 and F3) relative to nonacidified mesocosms (P0, P1 and P3). If this was the case, we should not expect to observe differences in bacterial assemblage structure between the three F mesocosms, which was in fact the case (Fig. 2 and Table 2). In addition, we might expect low or no bacterial production in the F mesocosms because of inhibition of heterotrophic carbon assimilation and, subsequently, growth. Bacterial production measured by ^{3}H-leucine incorporation reached a maximum of ~2.2 μg C L^{-1} in the F3 mesocosm on Day 7 (Supporting Information, Fig. S1), providing strong evidence for heterotrophic production and bacterial growth under acidified conditions. Similary, we observed decreasing phosphate turnover rates over time in all mesocosms (Fig. S2), but particularly in those amended with glucose, suggesting that all mesocosm bacterial assemblages had become nutrient-limited over time as a consequence of growth.

Although the taxonomic composition of our samples is in good agreement with previously published studies of seawater samples and the effects of glucose manipulation on marine bacterial assemblages (Eilers *et al.*, 2000b; Øvreås *et al.*, 2003; Witt *et al.*, 2011), we cannot conclude with certainty that all bacterial taxa have been detected (Fig. 2 and Table 1). It is possible that other significant bacterial assemblage shifts occurred in the mesocosms, but that neither the depth of sequencing used here, nor the temporal or taxonomic resolutions were sufficient to reveal them. We cannot exclude the possibilities that certain OTU have skewed representation in our data sets because of PCR amplification or rRNA gene copy bias (Crosby & Criddle, 2003; Sipos *et al.*, 2007), or that incubation effects associated with seawater mesocosms may have induced false shifts in the natural microbial assemblages (Ferguson *et al.*, 1984; Fuchs *et al.*, 2000; Massana *et al.*, 2001). Despite these points of caution, however, the present experimental results identify future avenues of investigation for increasing understanding of the biological pump and its vulnerability to ocean acidification.

The experimental set-up precluded our ability to sample from true biological replicates for pyrosequencing analyses of bacterial assemblages. Replicate mesocosms have been found to hardly diverge across time (Martínez-Martínez *et al.*, 2006) leading us to the believe that the strong response in the mesocosm bacterial assemblages to high glucose addition at the present pCO_2 level and subsequent elimination of this response at elevated pCO_2, as reported in this study, are real. Given the relevance of the signal, however, we want to highlight a need for mesocosm experiments with replication on this topic to corroborate our findings as well as replication of this mesocosm experiment itself both in the Arctic Ocean and in other waters to gain a more holistic picture of the interactive effects of glucose and pCO_2 in marine systems.

Acknowledgements

The authors would like to thank Jorun K. Egge for sample preparation and Michael Dondrup for assistance with PERL scripts. Financial support was provided by the Norwegian Research Council NORKLIMA project 'Marine Ecosystem Response to Climate Change' (MERCLIM, project number 184860/S30), by the French Agence Nationale de la Recherche (ANR) AQUAPHAGE program, and by the European Research Council Advanced Grant ERC-AG-LS8 'Microbial Network Organisation' (MINOS, project number 250254). The authors wish to dedicate this article to the memory of Runar Thyrhaug.

References

Allers E, Gómez-Consarnau L, Pinhassi J, Gasol JM, Simek K & Pernthaler J (2007) Response of Alteromonadaceae and Rhodobacteriaceae to glucose and phosphorus manipulation in marine mesocosms. *Environ Microbiol* **9**: 2417–2429.

Alonso C & Pernthaler J (2006) Roseobacter and SAR11 dominate microbial glucose uptake in coastal North Sea waters. *Environ Microbiol* **8**: 2022–2030.

Alonso C, Warnecke F, Amman R & Pernthaler J (2007) High local and global diversity of Flavobacteria in marine plankton. *Environ Microbiol* **9**: 1253–1266.

Alonso-Sáez L & Gasol JM (2007) Seasonal variations in the contributions of different bacterial groups to the uptake of low-molecular-weight compounds in Northwestern Mediterranean Coastal waters. *Appl Environ Microbiol* **73**: 3528–3535.

Amon R (2004) The role of dissolved organic matter for the organic carbon cycle in the Arctic Ocean. *The Organic Carbon Cycle in the Arctic Ocean*, pp. 83–100. Springer-Verlag, Berlin/Heidelberg.

Andersson AF, Riemann L & Bertilsson S (2010) Pyrosequencing reveals contrasting seasonal dynamics of taxa within Baltic Sea bacterioplankton communities. *ISME J* **4**: 171–181.

Bano N & Hollibaugh JT (2002) Phylogenetic composition of bacterioplankton assemblages from the Arctic Ocean. *Appl Environ Microbiol* **68**: 505–518.

Bates NR & Mathis JT (2009) The Arctic Ocean marine carbon cycle: evaluation of air-sea CO_2 exchanges, ocean acidification impacts and potential feedbacks. *Biogeosciences* **6**: 2433–2459.

Bates DM, Mächler M & Bolker B (2012) Linear mixed-effects models using S4 classes. Available at: http://cran.r-project.org/web/packages/lme4/lme4.pdf

Beman JM, Chow C-E, King AL, Feng Y, Fuhrman JA, Andersson A, Bates NR, Popp BN & Hutchins DA (2011) Global declines in oceanic nitrification rates as a consequence of ocean acidification. *P Natl Acad Sci USA* **108**: 208–213.

Caldeira K & Wickett ME (2003) Oceanography: anthropogenic carbon and ocean pH. *Nature* **425**: 365.

Cole JR, Wang Q, Cardenas E *et al.* (2009) The Ribosomal Database Project: improved alignments and new tools for rRNA analysis. *Nucleic Acids Res* **37**: D141–D145.

Cottrell MT & Kirchman DL (2003) Contribution of major bacterial groups to bacterial biomass production (thymidine and leucine incorporation) in the Delaware Estuary. *Limnol Oceanogr* **48**: 168–178.

Crosby LD & Criddle CS (2003) Understanding bias in microbial community analysis techniques due to rrn operon copy number heterogeneity. *Biotechniques* **34**: 790–794.

Cuevas A, Egge JK, Thingstad TF & Töpper B (2011) Organic carbon and mineral nutrient limitation of oxygen consumption, bacterial growth and efficiency in the North Sea. *Polar Biol* **34**: 871–882.

Eilers J, Pernthaler J, Glöckner FO & Amann R (2000a) Culturability and *in situ* abundance of pelagic bacteria from the North Sea. *Appl Environ Microbiol* **66**: 3044–3051.

Eilers H, Pernthaler J & Amann R (2000b) Succession of pelagic marine bacteria during enrichment: a close look at cultivation-induced shifts. *Appl Environ Microbiol* **66**: 4634–4640.

Elifantz H, Malmstrom RR, Cottrell MT & Kirchman DL (2005) Assimilation of polysaccharides and glucose by major bacterial groups in the Delaware Estuary. *Appl Environ Microbiol* **71**: 7799–7805.

Engel A, Delille B, Jacquet S, Riebesell U, Rochelle-Newall E, Terbrüggen A & Zondervan I (2004) Transparent exopolymer particles and dissolved organic carbon production by *Emiliania huxleyi* exposed to different CO_2 concentrations: a mesocosm experiment. *Aquat Microb Ecol* **34**: 93–104.

Ferguson RL, Buckley EN & Palumbo AV (1984) Response of marine bacterioplankton to differential filtration and confinement. *Appl Environ Microbiol* **47**: 49–55.

Fuchs BM, Zubkov MV, Sahm K, Burkill PH & Amann R (2000) Changes in community composition during dilution cultures of marine bacterioplankton as assessed by flow cytometric and molecular biological techniques. *Environ Microbiol* **2**: 191–201.

Fuhrman JA, Steele JA, Hewson I, Schwalbach MS, Brown MV, Green JL & Brown JH (2008) A latitudinal diversity gradient in planktonic marine bacteria. *P Natl Acad Sci USA* **105**: 7774–7778.

Galand PE, Casamayor EO, Kirchman DL & Lovejoy C (2009) Ecology of the rare microbial biosphere of the Arctic Ocean. *P Natl Acad Sci USA* **106**: 22427–22432.

Gattuso J-P & Lavigne H (2009) Technical note: approaches and software tools to investigate the impact of ocean acidification. *Biogeosciences* **6**: 2121–2133.

Gontcharova V, Youn E, Wolcott RD, Hollister EB, Gentry TJ & Dowd SE (2010) Black Box Chimera Check (B2C2): a windows-based software for batch depletion of chimeras from bacterial 16S rRNA gene datasets. *Open Microbiol J* **4**: 47–52.

Hirche H-J, Baumann MEM, Kattner G & Gradinger R (1991) Plankton distribution and the impact of copepod grazing on primary production in Fram Strait, Greenland Sea. *J Mar Syst* **2**: 477–494.

Hornik K (2012) *The R FAQ*. Available at: http://cran.r-project.org/doc/FAQ/R-FAQ.html, Chapter 7.35.

Kirchman DL, Cottrell MT & Lovejoy C (2010) The structure of bacterial communities in the western Arctic Ocean as revealed by pyrosequencing of 16S rRNA genes. *Environ Microbiol* **12**: 1132–1143.

Kunin V, Engelbrektson A, Ochman H & Hugenholtz P (2010) Wrinkles in the rare biosphere: pyrosequencing errors can lead to artificial inflation of diversity estimates. *Environ Microbiol* **12**: 118–123.

Malmstrom RR, Cottrell MT, Elifantz H & Kirchman DL (2005) Biomass production and assimilation of dissolved organic matter by SAR11 bacteria in the Northwest Atlantic Ocean. *Appl Environ Microbiol* **71**: 2979–2986.

Malmstrom RR, Straza TRA, Cottrell MT & Kirchman DL (2007) Diversity, abundance, and biomass production of bacterial groups in the western Arctic Ocean. *Aquat Microb Ecol* **47**: 45–55.

Marie D, Brussaard CPD, Thyrhaug R, Bratbak G & Vaulot D (1999) Enumeration of marine viruses in culture and natural samples by flow cytometry. *Appl Environ Microbiol* **65**: 45–52.

Martínez-Martínez J, Norland S, Thingstad TF, Schroeder DC, Bratbak G, Wilson WH & Larsen A (2006) Variability in microbial population dynamics between similarly perturbed mesocosms. *J Plant Res* **28**: 783–791.

Massana R, Pedrós-Alió C, Casamayor EO & Gasol JM (2001) Changes in marine bacterioplankton phylogenetic composition during incubations designed to measure biogeochemically significant parameters. *Limnol Oceanogr* **46**: 1181–1188.

Nagata T (2008) Organic matter–bacteria interactions in seawater. *Microbial Ecology of the Oceans* (Kirchman DL, ed.), pp. 207–241. John Wiley & Sons, Inc., Hoboken, NJ.

Øvreås L, Bourne D, Sandaa R-A, Casamayor EO, Benloch S, Goddard V, Smerdon G, Heldal M & Thingstad TF (2003) Response of bacterial and viral communities to nutrient manipulations in seawater mesocosms. *Appl Environ Microbiol* **31**: 109–121.

Pinhassi J & Berman T (2003) Differential growth response of colony-forming α- and γ-proteobacteria in dilution culture and nutrient addition experiments from Lake Kinneret (Israel), the Eastern Mediterranean Sea, and the Gulf of Eilat. *Appl Environ Microbiol* **69**: 199–211.

Pinhassi J, Gómez-Consarnau L, Alonso-Sáez L, Pedrós-Alió C & Gasol JM (2006) Seasonal changes in bacterioplankton nutrient limitation and their effects on bacterial community composition in the NW Mediterranean Sea. *Aquat Microb Ecol* **44**: 241–252.

Pinheiro JC & Bates DM (2000) *Mixed-Effects Models in S and S-PLUS*. Springer, New York, NY.

Pommier T, Canbäck B, Riemann L, Boström KH, Simu K, Lundberg P, Tunlid A & Hagström Å (2007) Global patterns of diversity and community structure in marine bacterioplankton. *Mol Ecol* **16**: 867–880.

Pommier T, Neal PR, Gasol JM, Coll M, Acinas SG & Pedrós-Alió C (2010) Spatial patterns of bacterial richness and evenness in the NW Mediterranean Sea explored by pyrosequencing of the 16S rRNA. *Aquat Microb Ecol* **61**: 221–233.

R Development Core Team (2005) *R: A language and environment for statistical computing, reference index version 2.15.1*. R Foundation for Statistical Computing, Vienna, Austria. ISBN 3-900051-07-0, URL http://www.R-project.org.

Rich JJ, Duckow HW & Kirchman DL (1996) Concentrations and uptake of neutral monosaccharides along 140°W in the equatorial Pacific: contribution of glucose to heterotrophic bacterial activity and the DOM flux. *Limnol Oceanogr* **41**: 595–604.

Riebesell U, Schulz KG, Bellerby RGJ *et al.* (2007) Enhanced biological carbon consumption in a high CO_2 ocean. *Nature* **450**: 545–548.

Sandaa R-A, Gómez-Consarnau L, Pinhassi J, Riemann L, Malits A, Weinbauer MG, Gasol JM & Thingstad TF (2009) Viral control of bacterial biodiversity – evidence from a nutrient-enriched marine mesocosm experiment. *Environ Microbiol* **11**: 2585–2597.

Sipos R, Székely AJ, Palatinszky M, Révész S, Márialigeti K & Nikolausz M (2007) Effect of primer mismatch, annealing temperature and PCR cycle number on 16S rRNA gene-targetting bacterial community analysis. *FEMS Microbiol Ecol* **60**: 341–350.

Smith WO Jr & Nelson DM (1990) Phytoplankton growth and new production in the Weddell Sea marine ice zone in the austral spring and autumn. *Limnol Oceanogr* **35**: 809–821.

Tanaka T, Thingstad TF, Løvdal T *et al.* (2008) Availability of phosphate for phytoplankton and bacteria and of glucose for bacteria at different pCO_2 levels in a mesocosm study. *Biogeosciences* **5**: 669–678.

Thingstad TF, Hagström Å & Rassoulzadegan F (1997) Accumulation of degradable DOC in surface waters: is it caused by a malfunctioning of the microbial loop? *Limnol Oceanogr* **42**: 398–404.

Thingstad TF, Øvreås L, Egge JK, Løvdal T & Heldal M (2005) Use of non-limiting substrates to increase size; a generic strategy to simultaneously optimize uptake and minimize predation in pelagic osmotrophs? *Ecol Lett* **8**: 675–682.

Thingstad TF, Bellerby RGJ, Bratbak G *et al.* (2008) Counterintuitive carbon-to-nutrient coupling in an Arctic pelagic ecosystem. *Nature* **455**: 387–390.

Thingstad TF, Strand E & Larsen A (2010) Stepwise building of plankton functional type (PFT) models: a feasible route to complex models? *Prog Oceanogr* **84**: 6–15.

Toggweiler JR (1993) Carbon overconsumption. *Nature* **363**: 210–211.

Töpper B, Larsen A, Thingstad TF, Thyrhaug R & Sandaa R-A (2010) Bacterial community composition in an Arctic phytoplankton mesocosm bloom: the impact of silicate and glucose. *Polar Biol* **33**: 1557–1565.

Witt V, Wild C, Anthony KRN, Diaz-Pulido G & Uthicke S (2011) Effects of ocean acidification on microbial community composition of, and oxygen fluxes through, biofilms from the Great Barrier Reef. *Environ Microbiol* **13**: 2976–2989.

Supporting Information

Additional Supporting Information may be found in the online version of this article:

Fig. S1. Bacterial production in individual mesocosms over time as determined by measurement of ^{3}H-leucine incorporation according to the method of Cuevas *et al.* (2011).

Fig. S2. Phosphate turnover in individual mesocosms over time as determined by the ^{33}P-orthophosphate method described in Tanaka *et al.* (2008).

Table S1. Physicochemical parameters in the six experimental mesocosms on Day 9.

Please note: Wiley-Blackwell is not responsible for the content or functionality of any supporting materials supplied by the authors. Any queries (other than missing material) should be directed to the corresponding author for the article.